Preparation, Characterization and Photocatalytic Activities of TiO$_2$ towards Methyl Red Degradation

**AWARE DINKAR VISHWANATH[1], JADHAV SHRIDHAR SHANKAR[2]*,
NAVGIRE MADHUKAR EKNATH[3], ATHARE ANIL EKNATH[2] and KOLHE NITIN HARIBHAU[2]**

[1]Department of Chemistry, Arts, Commerce and Science College Sonai,
Tal. Newasa, Dist. Ahmednagar-414603, Affiliated to S.P. Pune University, India.
[2]P.G. Department of Chemistry, New Arts, Commerce and Science College,
Ahmednagar, 414001, Affiliated to S.P. Pune University, India.
[3]Jijamata College of Science and Arts, Bhende, Ahmednagar 414 605,
Affiliated to S.P. Pune University, India.
*Correspondant author E-mail: ssjadhav1957@gmail.com

ABSTRACT

Highly efficient, photoactive, nanocrystalline TiO$_2$ powder was prepared with the help of modified sol-gel method. The prepared nanomaterials were characterized by modern techniques such as, TG-DTA, XRD, FE-SEM, EDX, TEM, BET surface area and FT-IR analysis for the identification of phase structure, phase composition and morphology. Formation of thermally stable, nanocrystalline, highley photocatalytic active, tetragonal anatase Titania was confirmed by TGA-DTA, XRD and HR-TEM. Similarly, FE-SEM confirms spherical, cauliflower like morphology for all Titania samples prepared with different cationic surfactants. The presence of mesoporous Titania was also confirmed by N$_2$ adsorption-desorption. The effect of addition of various surfactants significantly improves the photocatalytic activity. Prepared nanomaterials were successfully tested under UV-Vis light region for photodegradation of Methyl Red (MR) dye material which is act as water pollutant. The C$_{16}$TAB assisted Titania exhibits enhance photocatalytic efficiency as compared to industrially applied photocatalyst, Titania (Degussa P25) and zinc oxide under similar experimental condition.

Keywords: TiO$_2$ nanoparticles; cationic surfactants: sol-gel synthesis; photocatalysis; methyl red.

INTRODUCTION

Removal of toxic and harmful organic effluents from environment using advanced oxidation process (AOP) has been attracted extensive attention in today's scientific world[1]. Semiconducting metal oxides like TiO$_2$, ZnO are most widely used for environmental remediation in heterogeneous photocatalysis[2, 3]. The Titania is important heterogeneous catalysts used for water

splitting reported by Honda and Fujishima[4]. Titania is most studied and used semiconducting photocatalyst in the field of heterogeneous photocatalysis due to its easily availability, nontoxicity, reusability and recyclability[5, 6]. Also its high chemical stability towards the photocorrosion and strong oxidizing property of holes produced by photons during photolysis are the most important advantages over commercially zinc oxide photocatalyst. The photocatalytic activity of Titania is mainly depends on its polymorphic form, crystallinity, particle size, surface area, surface adsorption-desorption and use of synthetic methodology[7, 8]. Out of three polymorphs, anatase is more photocatalytically active than rutile, but it is susceptible to thermal treatment and hence, get radially converted to most thermally stable photoinactive rutile polymorphs when calcined at higher temperature. The anatase Titania has wide band gap energy and therefore its photocatalytic applications are limited to 3-5% of visible light. Various synthetic methodology including hydrothermal, sol-gel, co-precipitation, combustion, sol-gel- auto-combustion, ultrasonic modified by sol-gel, microwave assisted sol-gel[9-12] are used for the preparation of nanocrystalline mesoporous anatase Titania nanomaterials. In most of the synthetic methods mineral acids, bases and costly hazardous organic reagents are used for the preparation of nanocrystalline, mesoporous, anatase Titania. The surfactant templates are mostly used to control the particle size, phase transformation and for improvement in the surface morphology like crystallinity and mesoporous properties of Titania. The cationic surfactant, cetyl trimethyl ammonium bromide (CTAB) is most widely used hydrothermal[13, 14] and sol-gel[8, 15] preparation of mesoporous Titania nanoparticles. CTAB is mostly used in the reduction of grain size and for stability of anatase polymorphic phase upon high temperature thermal treatment[16].

In this study we report the preparation of highly efficient, photoactive, nanocrystalline TiO_2 powder with the help of ultrasonic Sonicator. It was modified by using various surfactants and sol-gel method. After calcination at 500°C for 4 hours, were characterized using modern analytical techniques and tested for the photocatalytic degradation of Azo dye, methyl Red (MR). The photocatalytic application of prepared Titania nanoparticles were also simultaneously compared with commercial material like TiO_2 (Degussa, P-25) and ZnO using same parameters.
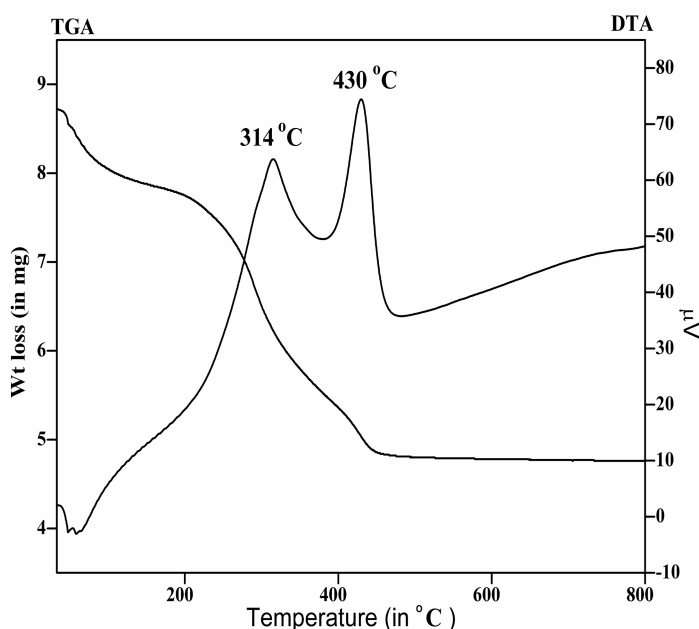

Fig. 1: TG-DTA graph of dried Titania before calcination

EXPERIMENTAL

Materials

A.R. grade chemicals were used for preparation without further purification. Titanium(IV) Butoxide [Ti(C$_4$H$_9$O)$_4$], cationic surfactants: i.e., Cetyl Ttrimethyl Ammonium Bromide (C$_{16}$TAB), Octadecyl Trimethyl Ammonium Bromide (C$_{18}$TAB), Cetyl Trimethyl Ammonium Chloride (CTACl) and Benzalkonium Chloride (BAC) were obtained from Sigma-Aldrich. TiO$_2$ (Degussa, P-25), Zinc oxide (ZnO), Isopropyl Alcohol [(CH$_3$)$_2$CHOH] and Methyl Red (MR) were received from SD Fine Chemicals Ltd, India, while Ethyl Alcohol is obtained from local alcohol distillery plant. All the experiments were done using double distilled deionized water as a solvent.

Preparation of TiO$_2$ nanoparticles

The preparation of Titania (TiO$_2$) was carried out by sol-gel method using water-alcohol mixture as a solvent. The procedure includes slow addition of Ethyl Alcohol (160 mL) and Isopropyl Alcohol (20 mL) with Titanium (IV) Butoxide (20 g) of under sonication at the temperature 40°C for 30 minutes. To this solution C$_{16}$TAB (2 g) surfactants in alcoholic condition was added. The resultant solution

was mixed with double distilled water (100 mL) under constant magnetic stirring (800 rpm) at 60°C for 4 hours and finally dried in oven for 12 hours at 110°C. Finally, the resultant dry powder was calcined at 500°C for 4 hours in muffle furnace under static air atmosphere. Similarly, all other TiO$_2$ nanomaterials were prepared only by changing the surfactant.

Characterization

The all prepared nanomaterials were characterized by sophisticated modified modern techniques such as, TG-DTA, XRD, FE-SEM and EDX, TEM, BET surface area and FT-IR analysis for the identification of phase structure, phase composition and morphology.

Photocatalytic Activity results of the Methyl Red (MR) Dyes

The photocatalytic degradation of MR dye was carried out in 250 ml double-jacket cylindrical reactor. The temperature of the reactor was controlled by circulating water around it. The photoreactor was set 30 cm away from the lamp. The irradiation was supplied by using metal halide bulb (Halonix, 400W). A catalyst (50 mg/L) is added in the MR dye solution (30 mg/L). Firstly, the dye solution with catalyst was
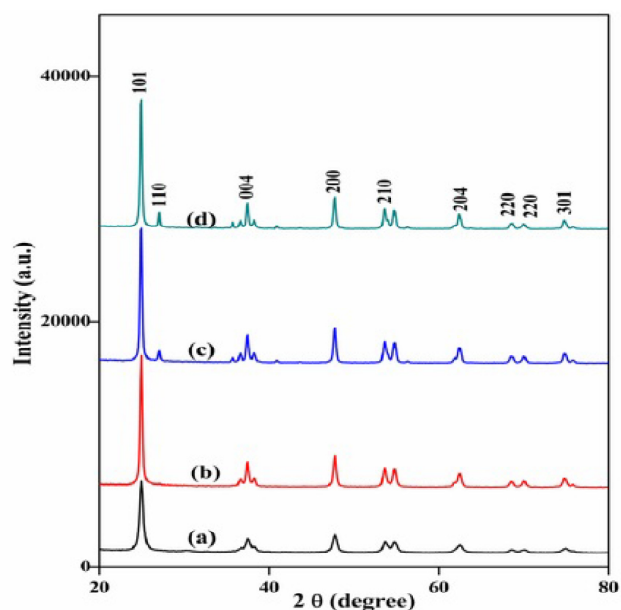

Fig. 2: XRD of Titania using cationic surfactants, (a) C$_{16}$TAB, (b) C$_{18}$TAB, (c) CTACl, and (d) BAC

dispersed by using ultrasonic sonicator and then stirred magnetically in in absence of light (dark) for 30 minutes to attain adsorption-desorption equilibrium. Immediately, light source was switch on, absorption of solution was measured at λ_{max} = 429 nm after the intervals of 15 min.

RESULTS AND DISCUSSIONS

TG-DTA Analysis

Figure 1 gives the TG–DTA graph of Titania. The DTA curve distinctly shows two exothermic peaks, the first peak at 314°C, is due to the decomposition of residual organic compounds and added surfactants during synthetic process. While the second sharp peak at 430°C is due to the crystallization of Titania[17, 18]. The TGA curve gives total weight loss upto 44.83 wt % and it was ended at 497.8°C. Thus the prepared dry material was calcined at the temperature 500°C for 4 hours.

XRD Analysis study

The XRD peaks prepared Titania samples were shown in **Figure 2**. All XRD confirms the formation of nanocrystalline, tetragonal anatase Titania as a major polymorph for all cationic surfactants. The diffraction pattern of Titania prepared using $C_{16}TAB$ and $C_{18}TAB$ shows diffraction peaks at 2q° = 25.3, 37.8, 48.0, 54.1, 67.7, 70.3 and 76.0 mainly for the crystal planes of (101), (004), (200), (210) (204), (220), and (301) and matching to the Anatase TiO_2 (JCPDS file 21-1272). In addition to tetragonal phase, XRD pattern for Titania with BAC and CTACl surfactant shows the presence of small fraction of Rutile phase (JCPDS No. 01-073-1765) may be due to the synthetic methodology used during the preparation of nanomaterials[15, 19].

The presence of pure anatase phase in case of both $C_{16}TAB$ and $C_{18}TAB$ samples can be explained by the fact that only anatase was already nucleated before calcination[20]. In other cases rutile phase was nucleated after the sol–gel process. The differences in phase of Titania, mainly due to the change in chemical structure and presence of counter ion on the surfactant used. The types of counter ion present in the surfactants controls the structure of the ionic micellar solution and the size of colloidal aggregates. The chloride ions gives more hydrated colloidal surface than the bromide ions[15]. Thus, the effect of the large bromide counter ion results in a delayed phase transition from anatase
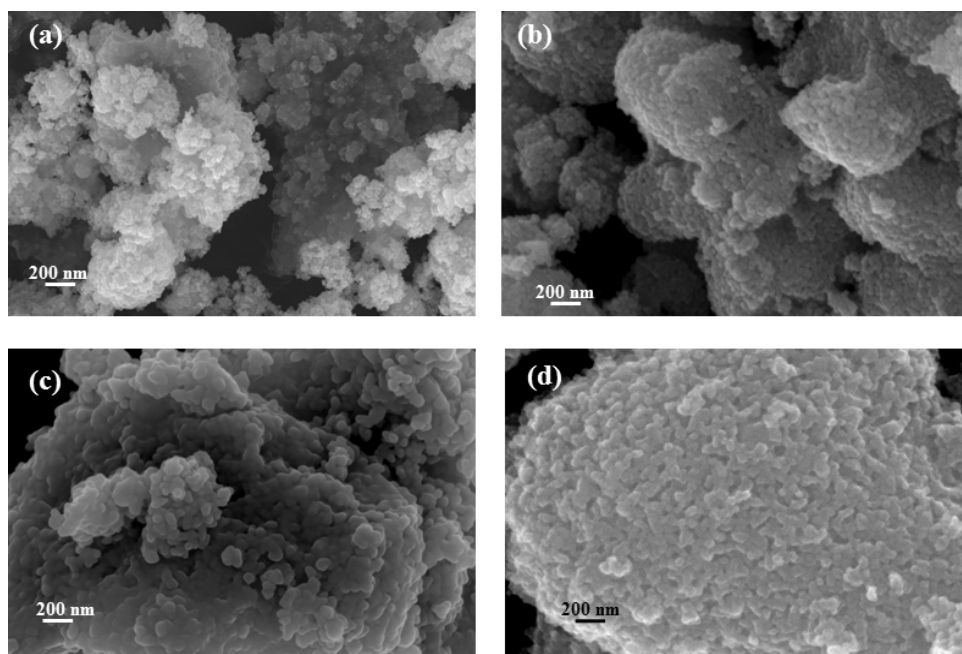

Fig. 3: FESEM photographs of Titania using cationic surfactants, (a)C_{16}TAB, (b)C_{18}TAB, (c) BAC, and (d) CTACl

to rutile and in the stabilization of the anatase phase during preparation of Titania.

Using Debye–Scherrer equation, the crystal size was calculated from the most intense peak (101),

$$D = \frac{K\lambda}{\beta \cos \theta}$$

Where, D= Average Crystallite Size, K= 0.89, ë= 0.15406 nm (Cu Ka), λ=FWHM, and θ= Diffraction Angle. The calculated values of crystal size were found in the range of 18.1-31.5 nm listed in the Table 1. The percent of Rutile fraction present in Titania was also calculated by following equation[22]

% Rutile = $[1+ 0.8 \, I_A/I_R]^{-1} \times 100$

Where, I_A=Integrated Intensity of Anatase (101) phase, I_R=Integrated Intensity of Rutile (110) phase. The calculated values of Anatase and Rutile percentages are also shown in Table 1. The results show that negligible proportion of Rutile is observed for Benzalkonium chloride (BAC) and hexadecyl trimethyl ammonium chloride (CTACl) surfactants.

FESEM and EDS Analysis

The FESM analysis shown in Figure 3 gives spherical nanoparticles with cauliflower-like aggregates. The aggregation is usually observed due the agglomeration of nanoparticles with average grain size below 50 nm[15].

The elemental composition of the prepared Titania nanoparticles using C_{16}TAB surfactant was given in the Figure 4. EDX spectrum represents the presence of proper proportion of Ti and O elements in prepared nanomaterials (Inset Fig. 4)

TEM and HRTEM study

Figure 5 (a, b) gives the TEM photographs of Titania prepared using C_{16}TAB at different resolutions. TEM images show regular spherical likes morphology with average particle diameter in the range of 18-20 nm which gives similar in size already discussed in XRD study shows crystallite size with 18.1 nm. HRTEM image shown in Figure 5 (c) gives the existence of clear lattice fringes which (lattice spacing of 0.356 nm) confirms the formation of highly crystalline mesoporous anatase Titania nanoparticles. The SAED pattern of pure Anatase phase for Titania shown in Figure 5(d). The indexed SAED pattern confirms the formation of Anatase Titania, also there is no any evidence of rutile phase (JCPDS card no. 21-1272).

BET Surface Area study

Figure 6 shows the nitrogen adsorption-desorption isotherm of representative sample, C_{16}TAB -TiO_2. It shows a type IV isotherm, which is typical for mesoporous materials. The BET specific surface area was found to be 43.4 m^2/g, which is higher than non-porous TiO_2 materials (2-30 m^2/g). Average pore diameter was obtained from BJH analysis and was found to be 2.1 nm.

FT-IR Analysis

Figure 7 shows FTIR spectrums of Titania nanoparticles prepared using different cationic surfactants. FTIR spectrum for O-H stretching vibrations shows a broad spectrum in the range of 3299-3415 cm^{-1}. Amount of O-H groups adsorbed on the surface of catalyst are responsible for enhancing the photocatalytic efficiency. The C_{16}TAB assisted Titania exhibits highest peak intensity and it goes on decreasing from C_{16}TAB to BAC. A sharp peak observed at 1636–1656 cm^{-1} corresponds to the

Table 1: Crystallite size calculated by using Debye- Sheerer equation

No.	Surfactant	Crystallite size (nm)		% Anatase	% Rutile
		Anatase	Rutile		
1.	C_{16}TAB	18.1	-	100	-
2.	C_{18}TAB	22.6	-	100	-
3.	CTACl	22.9	31.5	92	08
4.	BAC	31.3	31.3	88	12

H_2O adsorbed on surface gives bending vibrations of H-O-H group[23]. A very weak band in the range 1324-1390 cm^{-1} is also seen in the FTIR spectra, which is due to the C-H vibrations of surfactants, existence of these peaks shows proper capping of Titania with different surfactants during preparation process[24]. A broad peak seen in the range between 581–918 cm^{-1} were due to the vibrations of six co-ordinated TiO_6 octahedron and four coordinated Ti-O starching of anatase titania.
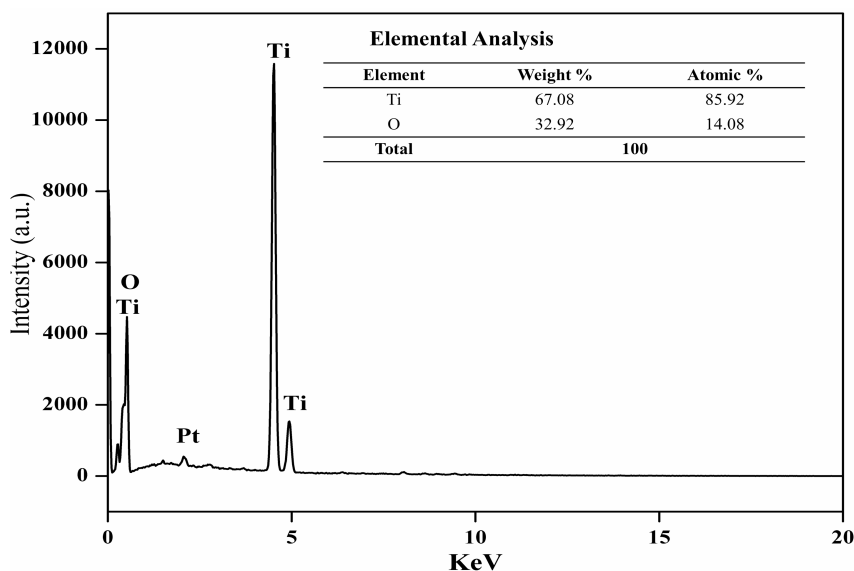

Elemental Analysis

Element	Weight %	Atomic %
Ti	67.08	85.92
O	32.92	14.08
Total		**100**

Fig. 4: EDS spectra of Titania using C$_{16}$TAB
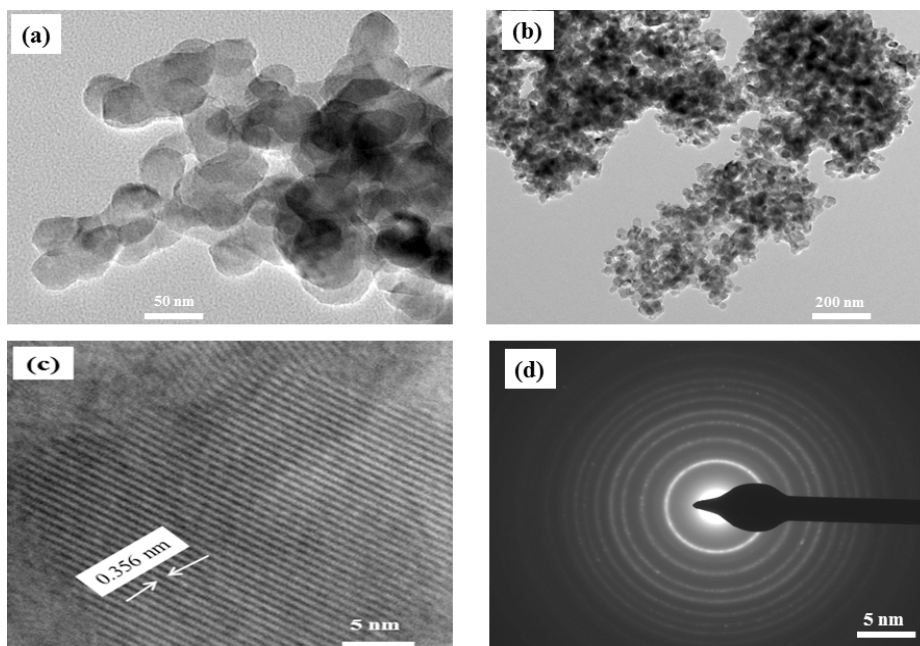
Fig. 5: TEM and HRTEM photographs of C$_{16}$TAB assisted TiO$_2$ nanoparticles (a, b) TEM images at different magnification, (c) HRTEM image, and (d) SAED pattern of anatase titania

Photocatalytic Activity Result

Photocatalytic efficiency of nanocrystalline titania was examined for photodegradation of methyl red (MR) at λ_{max} = 429 nm under UV-visible using spectrophotometer. Figure 8 shows absorption spectra of TiO_2 with different cationic surfactants. Interestingly, it was observed that concentration of dye goes on decreasing on exposure of time and most efficient catalytic performance (95.0 %) was recorded for Titania nanoparticles prepared using
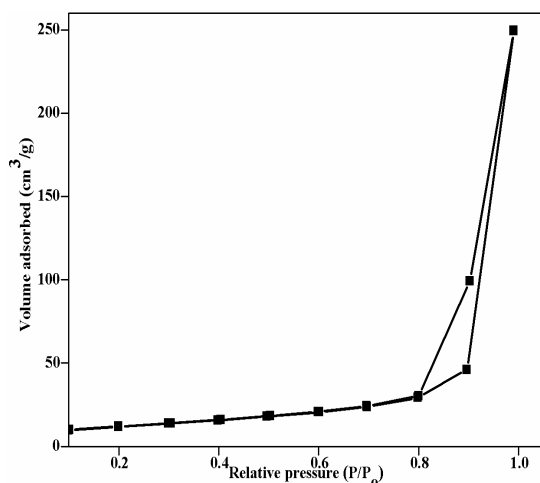
$C_{16}TAB$ and order of photodegradation efficiency was found to be, $C_{16}TAB > C_{18}TAB > CTACl > BAC$ upon 120 minutes light exposure time. Small grain size, nanocrystalline nature of pure anatase Titania prepared using $C_{16}TAB$, results high photocatalytic activity and further decrease in the photocatalytic efficiency is due to the increase in grain size with
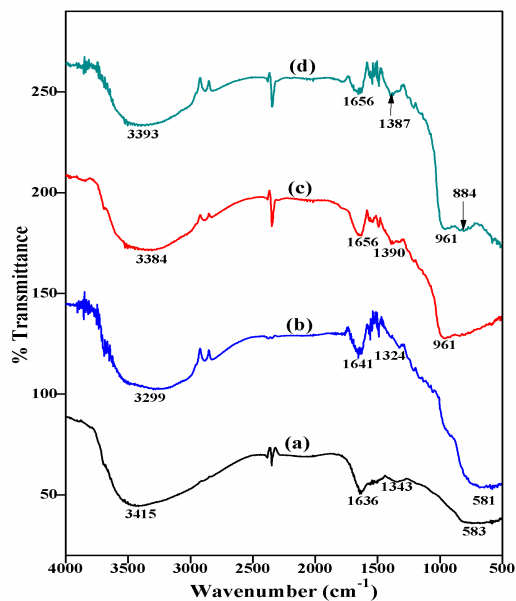

Fig. 6: N$_2$ Adsorption–Desorption isotherms of C$_{16}$TAB assisted Titania

Fig. 7: FT-IR spectrum of TiO$_2$ using different surfactants, (a) C$_{16}$TAB, (b) C$_{18}$TAB, (c) CTACl, and (d) BAC
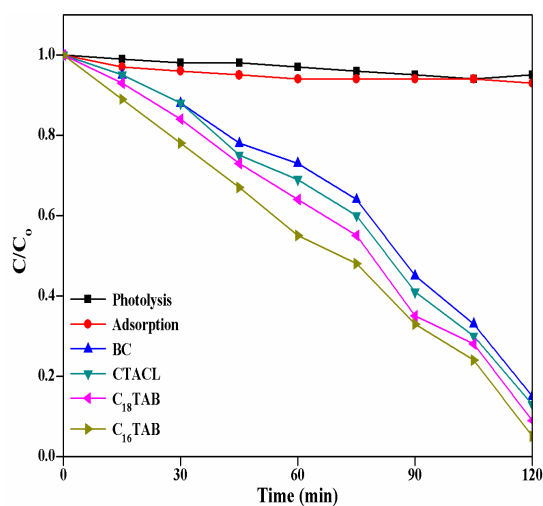

Fig. 8: Photodegradation of MR over TiO$_2$ prepared using various cationic surfactants
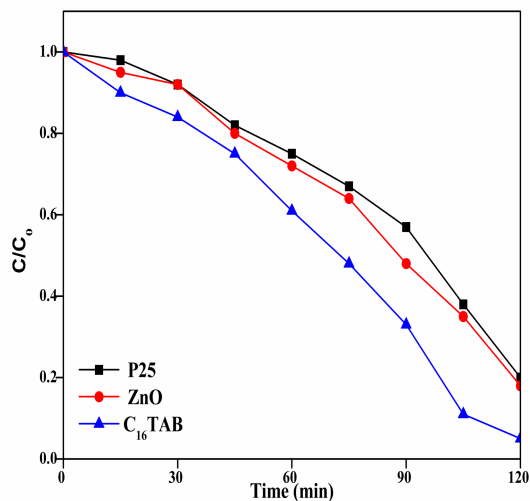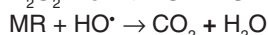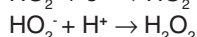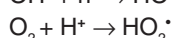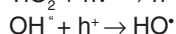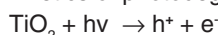

Fig. 9: Comparison of Photodegradation of MR over C$_{16}$TAB assisted TiO$_2$ and commercially available photocatalyst

partial phase transformation (anatase to rutile). Efficient photocatalytic activity is also confirmed from results of powder XRD, HRTEM and BET analytical results. The small grain size with nanocrystalline nature and mesoporous property of pure anatase Titania, lowers the recombination of e-/h+ and favors the formation of •OH radicals for better photocatalytic activity.

Under similar experimental condition prepared TiO_2 (C_{16}TAB) nanomaterials gives better activity as compare with commercially available photocatalyst TiO_2 (Degussa, P-25) and ZnO shown in Figure 9.

The probable reaction mechanism and kinetics of photodegradation of MR

$TiO_2 + h\nu \rightarrow h^+ + e^-$
$OH^{"} + h^+ \rightarrow HO^•$
$O_2 + H^+ \rightarrow HO_2^•$
$HO_2^• + e^- \rightarrow HO_2^-$
$HO_2^- + H^+ \rightarrow H_2O_2$
$H_2O_2 + e^- \rightarrow HO^- + HO^•$
$MR + HO^• \rightarrow CO_2 + H_2O$

Reaction kinetics of photodegradation of MR shows first order kinetics Langmuir Hinshelwood model,

$Ln (C_o/C_t) = k \times t$

C_o – Concentration at zero time and C_t - Concentration at t time

Order of reaction was found to be 0.029 min^{-1}, confirms the pseudo- first order kinetics mechanism.

CONCLUSION

With the use of modified sol-gel synthetic methodology, nanocrystalline Titania powder has been successfully prepared with help of different cationic surfactants considering their chain length and counter ions (chloride/bromide). The results of XRD and HRTEM confirm the formation of nanocrystalline, mesoporous anatase Titania polymorphs for C_{16}TAB and C_{18}TAB surfactants. While in case of CTACl and BAC, presence of highly reactive chloride counter ion facilitates quick hydrolysis of Titania precursor which results the increase in the grain size and anatase to rutile phase transformation. Titania nanoparticles prepared using C_{16}TAB shows best photocatalytic performance (95%) for MR dye degradation due to its smallest chin length and presence of bulkier bromide counter ion in its structure which slows the rate of hydrolysis of titania precursor. It can be concluded that Titania nanoparticles prepared using C_{16}TAB can be used for treatment of toxic environmental pollutants and industrial wastewater.

REFERENCES

1. Chan, S. H. S. ; Wu, T. Y., Juan , J. C. ; The, C. Y. *J. Chem. Technol. Biotechnol*. **2011,** *86,* 1130–1158.
2. Pelaez, M.; Nolan N. T.; Pillai, S. C.; Seery, M. K.; Falaras, P. A. ; Kontos G., Dunlop, P. S. M. ; Hamilton, J. W. J. ; Byrne J. A.; Shea, K. O. Entezari, M. H.; Dionysiou, D. D. *Appl. Catal. B Environ*. **2012** , *125*, 331–349.
3. Udom, I.; Ram, M. K.;Stefanakos, E. K.;Hepp, A. F.; Goswami, D. Y. *Mater. Sci. Semicond.*
Process. **2013,** *16,* 1–14.
4. Fujishima, K. A.; Honda, A. Nature. **1972**, *238*, 37-39.
5. Han, F.; Kambala, V. S. R.; Srinivasan, M. ; Rajarathnam, D. ;. Naidu, R "Appl. Catal. A Gen. **2009**, *359,* 25–40.
6. Malato, S.;Fernández-Ibáñez, P. ; Maldonado M. I.; Blanco, J.; Gernjak, W. *Catal. Today*, **2009**, *147*, 1–59.
7. Hanaor , D. A. H.; Sorrell, C. C. *J. Mater. Sci.*,

2011*, 46,* 855–874.

8. Shibata, H. T.; Ogura, T. ; Mukai, T.; Ohkubo, H.; Sakai; Abe, M. *J Am Chem Soc.* **2005,** *1127*, 6396–16397.

9. Rashad, M. M.; Shalan, A. E. *J. Mater. Sci. Mater. Electron.* **2013** *, 24*, 3189–3194.

10. Han, C.; Lee, H.; Han, S. *Bull. Korean Chem. Soc.* **2008***, 29*, 1495–1498.

11. Awati P. S.; Awate, S. V.; Shah, P. P.; Ramaswamy, V. *Catal. Commun.***2003***, 4,* 393–400.

12. Joo, J.; Kwon, S. G.; Cho, T.; Lee, Yu, M. J.; Yoon, J. *. Phys. Chem. B.* **2005***, 109* (32), 15297–15302

13. Li, R.; Dong, G.; Chen. G. *New J. Chem.* **2015**, *39*(9), 6854–6863.

14. Tian, G.; Fu, H.; Jing, L.; Xin, B. K.; Pan, L. S. *Phys. Chem. C.* **2088** *, 112,* 3083–3089.

15. Casino, S.; Lupo F. Di,; Francia, C. A.; Tuel,; Bodoardo, S.; Gerbaldi, C. *J. Alloys Compd.* **2014,** *594*, 114–121.

16. Tian, G.; Fu, H.; Jing, L.; Tian, C. *J. Hazard. Mater.* **2009***.161*(2-3),1122–1130.

17. Sreethawong, T. ; Suzuki, Y.; Yoshikawa, S. *J. Solid State Chem.***2005,***178*, 329–338.

18. Mayo, M. J. *J. Am. Ceram. Soc.* **1957**, *77,* 1957–1960.

19. Yang, Z.; Choi, D.; Kerisit, S.; Rosso K. M.; Wang D.; Zhang, J.; Graff, G.; Liu, J. *J. Power Sources.* **2009**, *192*, 588–598.

20. Ovenstone J.; Yanagisawa, K. *Chem. Mater.* **1999**, *11*, 2770–2774.

21. Aswal V. K.; Goyal, P. S. *Chem. Phys. Lett.* **2003**, *368*, 59–65.

22. Spurr , R. A. ; Myers, H. *ACS Publ.* **1957,** *29,* 760–762.

23. Xiong, L.; Chen, C.; Chen, Q.; Ni, J. *J. Hazard. Mater.* **2011,** *189*(3), 741–748.

24. Manorama, S. V.; Reddy, K. M.;Reddy, C. V.; G., Narayanan, S.;Raja, P. R.; Chatterji, P. R. *J. Phys. and Chem. of solids*, **2002**, *63*, 135–143.